Earth Fissures in Wadi Najran, Kingdom of Saudi Arabia

Ahmed M. Youssef, Abdullah A. Sabtan, Norbert H. Maerz & Yasser A. Zabramawi

Natural Hazards
Journal of the International Society for the Prevention and Mitigation of Natural Hazards

ISSN 0921-030X

Nat Hazards
DOI 10.1007/s11069-013-0991-5

Nat Hazards
DOI 10.1007/s11069-013-0991-5

ORIGINAL PAPER

Earth Fissures in Wadi Najran, Kingdom of Saudi Arabia

Ahmed M. Youssef · Abdullah A. Sabtan · Norbert H. Maerz · Yasser A. Zabramawi

Received: 8 September 2012 / Accepted: 4 December 2013

Abstract The formation of earth fissures due to groundwater depletion has been reported in many places in North America, Europe, and Asia. Najran Basin is in the southern part of the Kingdom of Saudi Arabia, and agricultural activities and other groundwater uses have caused significant groundwater depletion there. The basin recently experienced a sudden appearance of numerous earth fissures. An interdisciplinary study consisting of an evaluation of land-use changes, and hydrological, hydrogeological, and geophysical investigations was conducted to determine the reason for the formation of the earth fissures. The hydrological analysis strongly revealed that the groundwater level is decreasing with time. Groundwater depletion would lead to the accumulation of subsurface stress, causing soil hydro-consolidation which creates the ideal condition for the formation of earth fissures. Electrical resistivity, data indicated that there are anomalies in the profiles, which are most probably due to the presence of subsurface topography, another key factor for the formation of the earth fissures.

Keywords Earth fissures · Water depletion · Najran · KSA

A. M. Youssef (✉) · Y. A. Zabramawi
Geological Hazards Department, Applied Geology Sector, Saudi Geological Survey, P.O. Box 54141, Jeddah 21514, Kingdom of Saudi Arabia
e-mail: amyoussef70@yahoo.com

A. M. Youssef
Geology Department, Faculty of Science, Sohag University, Sohag, Egypt

A. A. Sabtan
Geological and Environmental Engineering Department, Faculty of Earth Sciences, King Abdulaziz University, Jeddah, Kingdom of Saudi Arabia

N. H. Maerz
Geological Engineering Program, Missouri University of Science and Technology, Rolla, MO 65409-0660, USA

1 Introduction

Najran basin is in the extreme southwestern part of the Kingdom of Saudi Arabia (KSA). It is bordered to the east by the Empty Quarter Desert, the Asir region to the west, Ar-Riyadh and the Eastern Province in the north, and the Republic of Yemen to the south (Fig. 1). It is a vast area of about 360,000 km^2 with an estimated population of about 449,168 people. Najran basin, like other areas in the KSA, has experienced substantial development in the past 30 years from both the government and the private sector. The area includes many archeological sites, but is chiefly an agricultural area in the flood plain of Wadi Najran.

Najran basin and more specifically the area surrounding the city of Najran, experienced the appearance of several earth fissures at the ground surface due to groundwater depletion. Water overpumping may create significant tension in subsurface zones and is believed to be the primary cause of soil compaction, and the tension would lead to large-scale surface subsidence and the creation of earth fissures. Earth fissures can damage roads, buildings, and other infrastructure (Arizona Land Subsidence Group 2007). While earth fissures are present at the surface in some areas, the tension-induced ground cracking required developing fissures also may be present without surface expression. A tension crack propagates upward, and once it reaches the surface, it becomes exposed to erosion and may develop with time into a large surface feature. A visible, large earth fissure enhanced by erosion is properly termed a fissure gully. Methods are needed to detect incipient earth fissures that are not yet exposed at the surface so that they can be effectively mapped and mitigated.

Groundwater mining (overpumping aquifers) is one of the main causes of ground subsidence and earth fissure. The impact of ground subsidence and fissures will increase if the withdrawal of groundwater exceeds the aquifer safe yield (Bouwer 1978). The concept of safe yield is defined as the maintenance of a long-term balance between the groundwater withdrawal and groundwater recharge (Sophocleous 2000). For example, the Picacho Basin in south-central Arizona contains more than 50 ground cracks that were formed due to groundwater mining from the aquifer for agricultural irrigation (Holzer 1984). The thickness of the aquifer is about 700 m, and the decline in the basin groundwater level reached as much as 100 m. Water pumping clearly increased after 1940, and an area of about 300 km^2 has been affected by vertical subsidence of as much as 3.8 m in the ground surface (Holzer et al. 1979; Laney et al. 1978).

Ground subsidence due to groundwater mining may create earth fissures across, which differential may occur. Such fissures resemble fault scarps of tectonic origin. Scarps suspected to be related to groundwater withdrawal may be more than 1 km long and more than 0.2 m high. The longest scarp associated with groundwater mining measured to date is 16.7 km long (Verbeek et al. 1979), and the largest height of scarp is 1 m (Reid 1973). Displacement across earth fissures caused by groundwater withdrawal often follows the trend of pre-existing tectonic faults (Elsbury and Van Siclen 1983).

The characteristics of the earth fissures related to groundwater withdrawal reported by Holzer (1984) are as follow:

1) The fissures form due to stress that develops in aquifer materials as they consolidate due to ground subsidence.
2) The earth fissures form from tensile stresses, and sometimes extend along the direction of existing faults.
3) The fissures may extend from tens of meters to several kilometers accompanied by a ground dilation of more than several millimeters or more.

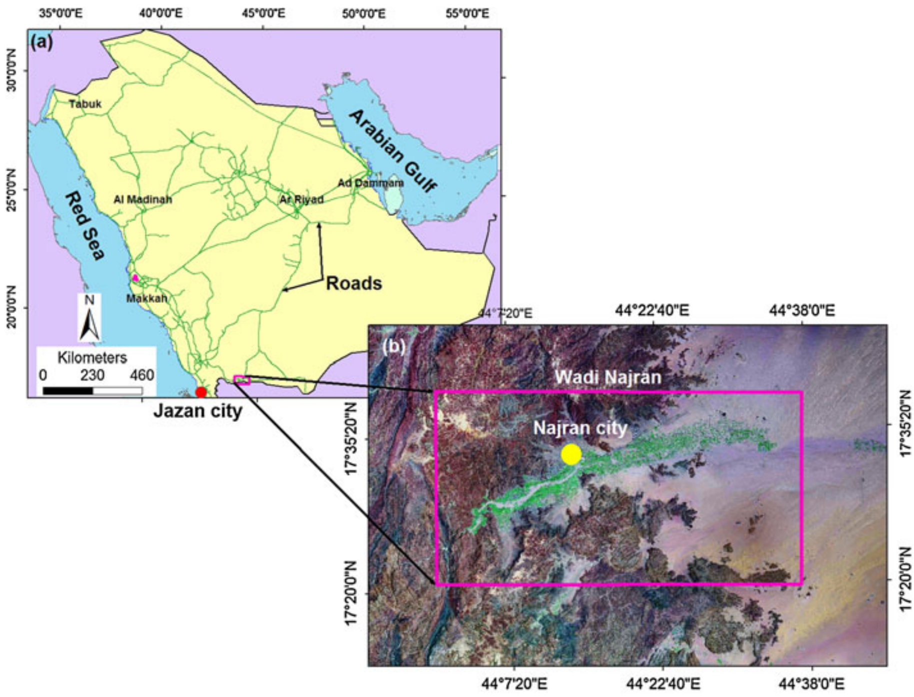

Fig. 1 Location of the Najran region in the KSA

4) Erosion processes increase the cracks width with time, and fissure gullies may reach 1–2 m wide and 2–3 m deep. The fissures appear at the surface, in some cases, with vertical offsets of more than 1 m along a distance of more than 16 km.
5) Vertical displacement across earth fissures may occur at rates of 4–60 mm/year, and most movement occurs when the soil is in the plastic range.

Many areas in the United States are affected by tension cracks or earth fissures associated with land subsidence due to groundwater mining (Holzer 1984). For example, subsidence of few centimeters to few meters due to groundwater extraction has occurred in Georgia, Louisiana, Texas, Nevada, and California (Poland 1981). Schumann (1995) indicated that earth fissures occur in three areas of differential subsidence on and near Luke Air Force Base, Arizona. He indicated that the subsidence led to flow reversal in a portion of the Dysart Drain, an engineered water conveyance structure; and that surface runoff from a four-inch rainfall event caused the drain to spill over, flooding the base runways, damaging more than 100 homes, and forcing the base to close for 3 days. In some cases, earth fissures may be kilometers long but only a few centimeters wide. However, once exposed at the ground surface, fissures are commonly eroded into gullies meters wide and meters deep. Ground subsidence and associated ground cracks or fissures represent a major problem in many countries of the world. Most of these fissures, cracks, and subsidence features are related to the vertical movement of the ground surface compared to the surrounding areas (Wittaker and Reddish 1989). The cracks begin as small traces that expand as a result of external factors such as living organisms and erosion due to the movement of surface water and rain. Sometimes they are located along the sides of the basins due to the presence of buried bedrock high below the basin sediments, or even due to a change in the nature of the soil. Some authors, such as Lofgren (1978) and Helm (1994) indicate that the ground cracks start from great depths below the surface, as a result of horizontal movement in the aquifers due to groundwater pumping from the unconsolidated aquifer layers.

Holzer (1984) reported a case of excessive groundwater pumping from a loose sediments aquifer, where the resulting ground subsidence damaged an area of 22,000 km^2 in the United States, and that subsidence was over 1 m in many areas. Sroka and Hejmanowski (1991) estimated geometrical changes on the surface and in the rock mass for deep extraction of solid, liquid, and gaseous minerals. Bell and Price (1993) indicated that hazards associated with earth fissures are generally more local and include damage to homes and buildings, roads, dams, canals, sewer and utility lines, as well as providing a conduit for contaminated surface water to rapidly enter groundwater aquifers. (Sun et al. 1999) reported a detailed case study of land subsidence due to groundwater withdrawal in southern New Jersey, USA. Mousavi et al. (2001) indicated that subsidence in the Rafsanjan Plain (about 900 km south of Tehran, Iran) is due to decline of groundwater levels. Wolkersdorfer Ch and Thiem 2006 studied groundwater withdrawal and land subsidence in northeastern Saxony, Germany. Ehret et al. (2007) produced another useful effort in this field by modeling the site effects of changing the groundwater level and derived theoretical formulae that calculate the change in the ground surface (subsidence). Xu et al. (2008) gave a general introduction to land subsidence prediction due to groundwater withdrawal in three regions in China (the deltaic plain of Yangtse River, North China Plain, and Fenwei Plain). They found that the subsidence zones in these regions are 2 m over an area of about 10,000 km^2 in the deltaic plain of Yangtse River, 3.9 m over an area of about 60,000 km^2 in the North China Plain, and 3.7 m over an area of about 1,135 km^2 in the Fenwei Plain. Lund et al. (2010) established draft recommendations and guidelines for land subsidence and earth fissure hazard investigations that may be applied to any project site, large or small. Zhang et al. (2010) indicated that several areas of land subsidence have been created due to the excessive groundwater withdrawal in the Su-Xi-Chang (SXC) area, China. Sahu and Sikdar (2011) come up with a new estimation of the rate of land subsidence, due to groundwater withdrawal, in and around Kolkata City and east Kolkata wetlands, West Bengal, India. They indicated that further over withdrawal of groundwater will result in continued land subsidence, and they estimated that the mean land subsidence rate is 13.53 mm/year, and for 1 m drop in the piezometric head, the mean subsidence is 3.28 cm.

2 Earth fissures in Saudi Arabia

Under arid desert conditions, it takes long years to recharge an aquifer. Groundwater mining, groundwater pumping in excess of aquifer recharge, may cause a continuous decline in groundwater levels in a relatively short period. When the aquifer is formed of porous, unconsolidated sediments and is inter-bedded with clay aquitards of low permeability and high compressibility, rapid lowering of the groundwater level may cause subsidence and possible ground failure in the form of earth fissures. It is known that land subsidence associated with mining of underground water from porous granular media is caused by a decrease in the volume of the reservoir system. As water is withdrawn from porous media, pore-water pressures decrease. Porous media deformation is controlled by effective stress (the difference between the total stress and pore-water pressure) and a decrease in pore-water pressure causes a decrease of pore volume (compaction phenomena). In other hand, the presence of aquitards both within and bounding the aquifer system is particularly prone to large compaction because of their compressibility. Typically, the compressibility (and therefore storability) of aquitards is several orders of magnitude larger than the compressibility of coarser-grained aquifers, which in turn is typically much larger than water compressibility. Accordingly, aquitard storability and drainage control the compaction of these aquifer systems and account for most of the land subsidence that accompanies groundwater development of these aquifer systems.

Spurred by rapid development in Saudi Arabia, excessive groundwater pumping is a common practice that has produced land subsidence and ground fissuring. Land subsidence and earth fissures are reported in several places and have caused agricultural, building, and infrastructure damage. Amin (1988) investigated the Tabah area, north of Hail, where he found some evidence of land subsidence, ground fissures, and differential displacement across earth fissures due to water depletion within an old volcanic crater. Further details were reported by Amin and Shehata (1991). Amin and Bankher (1995) indicated that groundwater mining in western Saudi Arabia caused sediments to hydro-consolidate, which is a form of geological hazard. For example, when floods covered Wadi Nafia and Wadi Alitma on January 31, 1992, the farmers discovered numerous ground cracks of different scales and orientation the next day (Bankher 1996). The cracks included over sixteen locations in an area 57 km south of the city of Medina and had a total length of 3,560 m.

3 Earth fissure problems

Earth fissures have suddenly appeared in agricultural and barren areas in the central part of the northern edge of Wadi Najran (Fig. 2). The affected area is privately owned and mainly used for agriculture. The earth fissures have various lengths; one of them extended in a northeast direction for a distance of 600 m and has widths that vary between 30 and 50 cm, and depths of 50–400 cm. The unexpected appearance of the earth fissures caused panic among the farmers and people in the area due to concern that the fissures might interfere with future land use.

4 Objectives

The main objective of this study was to figure out the causes and extent of the earth fissures in the Najran basin. We achieved this using three techniques: remote sensing, and hydrological and geophysical studies. Multitemporal resolution images including landsat multispectral scanner, landsat thematic mapper (TM), and enhanced thematic mapper plus (ETM+) were all used to map changes in land use over time. The hydrological part of the study estimated changes in groundwater level over time. The subsurface extent of earth fissures was explored by geophysical techniques.

5 Geomorphology and geology

From the analysis of satellite images and topographic maps, the study area can be divided into three geomorphological units: (1) high-mountain areas surrounding the region, (2)

Fig. 2 Fissuring associated with subsidence due to groundwater withdrawal in Najran (**a** and **b**) in an uninhabited area and (**c** and **d**) in agricultural fields

flood plain areas along the wadi, and (3) sandy dunes along the borders of the Empty Quarter. The highest point in the Empty Quarter region is 2,897 m above sea level. The rocks in the Najran area belong to the Proterozoic (Precambrian) era and consist of igneous rocks, as well as some stratified rocks of the Wajeed sandstone of Cambrian–Ordovician age, and occasional Tertiary bedrock (Sable 1985; Shanti 1993). Quaternary surficial materials include alluvial deposits of Wadi Najran and sand dunes mainly that located between Wadi Najran and the Empty Quarter.

6 Results and analysis

6.1 Land-use changes

Land-use planning provides a method for managing growth to obtain the maximum benefits from a limited resource. Development, no matter how respectful of nature, will cause an impact on the environment. Geologic hazards and resources must be recognized and evaluated, and the information derived from these evaluations is used to make intelligent decisions about land use for development. The study area has been subjected to land-use changes over the past few decades; in fact, some locations experienced substantial changes, especially regarding agricultural activities and residential expansion.

We used remote sensing techniques to delineate the changes that took place in the study area. Medrial et al. (2001) reported that vegetation indices are a combination of different spectral responses that come from the surface layer and are commonly used in the remote sensing studies. The indices are usually used to identify and evaluate the status of vegetation using visible, near infrared, and middle infrared regions of the electromagnetic spectrum. In the current study, we prepared a detailed land-use map by interpreting satellite images and making field investigations. We used the satellite images to evaluate land-use changes over the past 30 years, especially reclamation activities (desert lands converted to cultivated lands) by applying the normalized difference vegetation index (NDVI) aided by the Environment for Visualizing Images software (ENVI 4.5). These NDVI images were exported into ArcGIS 9.3 software, classified, and overlaid to create a composite final land-use map (Fig. 3). The data were essential in developing a series of different land-use maps to determine land-use changes over three time periods; before 1972, from 1972 to 1984, and from 1984 to 2001. The analysis showed that there has been a substantial increase in agricultural areas during the past few decades. In the same time period, there are also increase in the urban areas. The area covered by agricultural activities was limited to about 47 km^2 before 1972. From 1972 to 1984 agricultural area nearly doubled increasing by an additional 46 km^2. Finally, the increase in the agricultural areas from 1984 to 2001 was about 19 km^2.

6.2 Hydrological studies

6.2.1 Groundwater level decline

The major aquifer in the study area is the upper basin-fill unit. The thickness of sand and gravel deposits within this unit generally varies between 10 and 60 m, though in some places the thickness is much less, down to about 1.5 m. Determination of the lateral extent of water-bearing strata is very difficult due to the wide spacing of water wells and lateral variation of the water-bearing sand and gravel units. The aquifer in the unconsolidated basin-fill alluvium is generally unconfined (water-table aquifer). Seven water wells, which were drilled long time ago and still in use along Wadi Najran from west to east, have been used in the current study (Fig. 4). Historical water levels as well as recent measurements are available. When the recent and past measurements were compared, it was clear that groundwater levels in Wadi Najran decreased dramatically in the past decade (Fig. 5). This indicates that the water pumping in the valley was at a very high rate, much higher than the annual groundwater recharge to the aquifer. This explains the reason behind the continuous decrease of groundwater levels, which resulted in the dewatering of more than 1,000 wells.

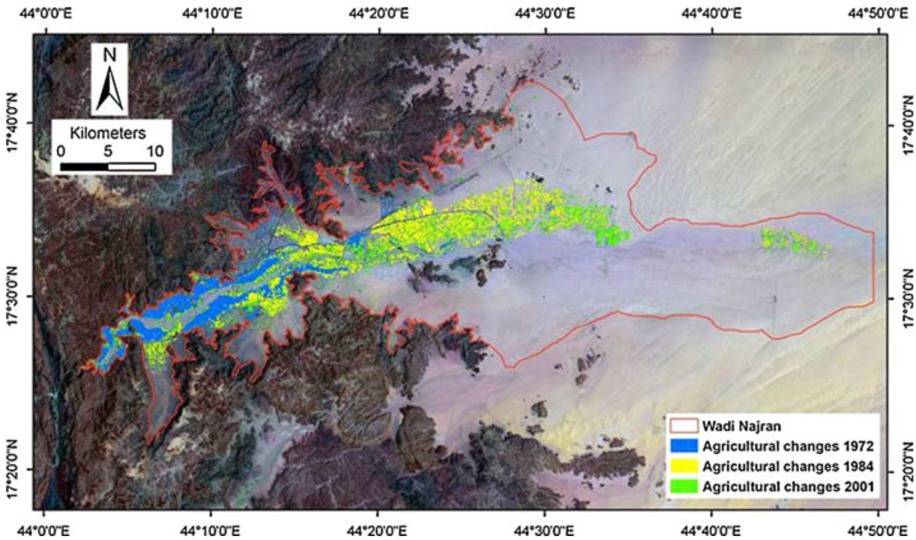

Fig. 3 Final land-use changes model in the study area draped over the ETM image bands 742 in RGB

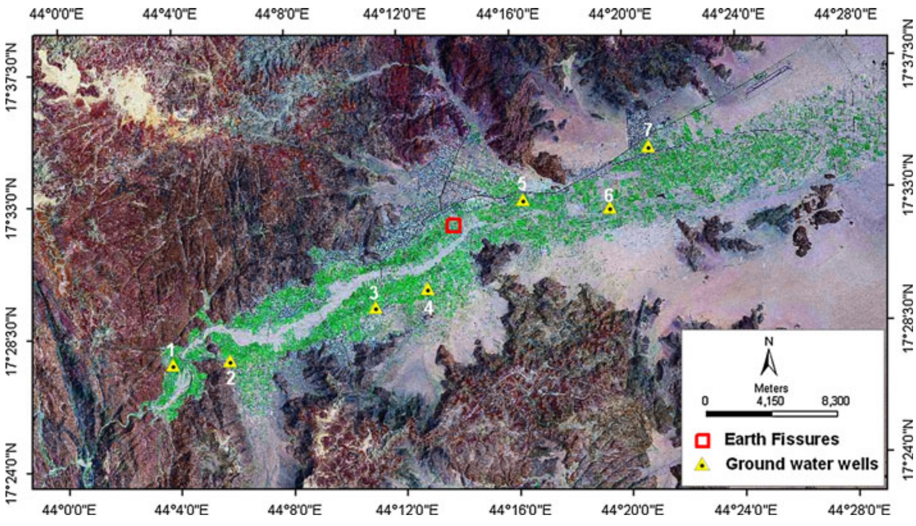

Fig. 4 Location of the water wells along Wadi Najran to used measure the groundwater level

6.2.2 Recharge calculation of Wadi Najran

Land use in the Najran area was limited before 1972, but the Kingdom has seen extensive development since the mid-seventies, and the study area is no exception. New settlers were attracted from the surrounding areas, and as their quality of life improved, it led to a huge rise in water demand. Excessive water pumping caused concentrated salts of halite, gypsum, calcite, and dolomite to be deposited between soil grains due to the evapotranspiration and upward movement of groundwater along the valley. Most of the groundwater in

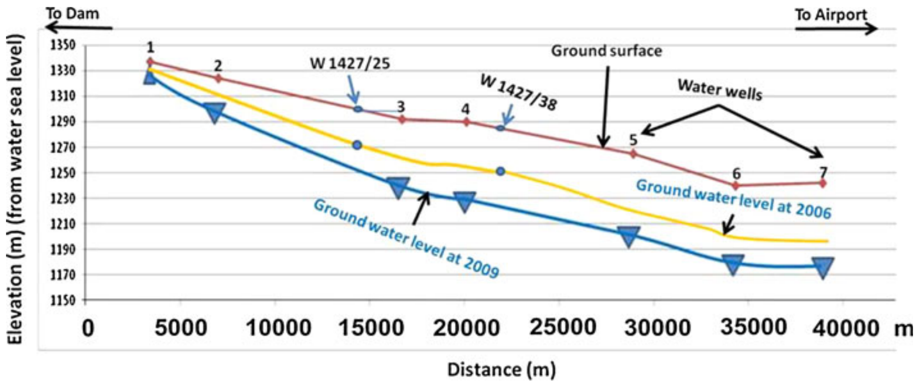

Fig. 5 Groundwater levels in the wells along Wadi Najran between 2006 and 2009

the study area is used for irrigation, but a minor part is for domestic consumption. With the absence of water management and conservation, it is risky to continue the present human activities in Wadi Najran without comparing aquifer natural recharge to the present water discharged, which is an important step toward appropriate water management. The average annual amount of rainfall in the present arid conditions for Wadi Najran is 70 mm/year.

The chloride mass balance technique was found to be easy to use and compatible with the hydrological conditions of arid to semiarid areas, which is the case in Najran region, to quantify groundwater recharge (Vacher and Ayers 1980; Alyamani and Hussein 1995). The method requires a simple measurement of the chlorine ion concentration in rain water, which is then compared to the chlorine value obtained from local wells. It is possible that the concentration of chlorine increases in groundwater due to salt deposition as a result of evaporation and/or is affected by agricultural fertilization. To avoid contamination, the water samples were taken from wells at the extreme upstream end of the Wadi Najran, and the following equation has been applied to determine the recharge of the aquifer (Rgw) mm/year.

$$\text{Rgw} = \left[\text{Pyr}\frac{\text{Clp}}{\text{Cl gw}}\right] \tag{1}$$

where Rgw is the recharge value (mm/year), Pyr is the amount of annual precipitation (mm), Clp is the chlorine ion concentration in rain water (mg/l), and Clgw is the chlorine ion concentration in groundwater (mg/l).

The Clp and Clgw values are 13 and 53 mg/l, respectively, for Wadi Najran. The calculated recharge value based on Eq. (1) is 17 mm/year. This value is equivalent to 24.3 % of the average annual precipitation for the study area.

The Najran aquifer recharge basin has a total area about 5,915 km^2. The basin area is arbitrarily divided into two parts; an area upstream of Najran dam, which has an area of about 4,800 km^2, and Wadi Najran itself downstream of Najran dam (1,115 km^2). The recharge calculation was carried out for each part separately as follow:

1. The water recharge for the area upstream of Najran dam (Fig. 6a) was calculated using Eq. (2).

$$\text{Recharge 2} = \text{Pyr*Awc} \tag{2}$$

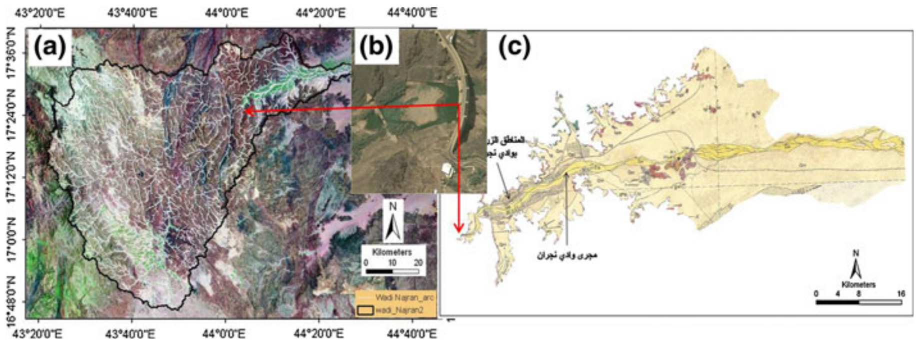

Fig. 6 **a** Najran basin, **b** Najran dam, and **c** Wadi Najran area downstream of the dam

where Pyr is the amount of annual precipitation (mm), Awc is the Wadi Najran basin area upstream of the Najran dam.

Based on Eq. (2), the precipitation is 3.32×10^8 m^3/year. It is assumed that out of the water that flows in Wadi Najran channel only 10 % of that water will infiltrate downward to the aquifer (based on field investigations). Then, the calculated recharge is 33.2×10^6 m^3/year.

2. Precipitation in Wadi Najran itself (downstream of the Wadi Najran dam (Fig. 6b, c), recharge was calculated using Eq. (3).

$$\text{Recharge } 1 = \text{Rgw}*\text{Awd} \quad (3)$$

where Rgw = recharge value (mm/year) and Awd = Wadi Najran area downstream of the Najran dam.

The recharge from the direct rains above the Wadi Najran, according to the Eqs. (1) and (3), can be estimated to be 1.9×10^7 m^3/year.

The total recharge for the Wadi Najran, Eq. (1) and (2), which is about 5.3×10^7 m^3/year.

6.2.3 Discharge calculation for Wadi Najran

Based on a field survey and preliminary information from the water agency in Najran, Wadi Najran has about 1,100 producing wells (for irrigation and domestic use). The average water pumping rate for irrigation was estimated in the field to be about 0.5 cubic meters per minute, for 7 h per day for each well. Some of these wells are for domestic use, and water is pumped from them using huge water-tank trucks. The estimated pumping rate is one cubic meter per minute for at least 14 h per day. Therefore, the total water discharge of the aquifer is about 84.3×10^6 m^3/year.

6.2.4 Recharge/discharge relationship

From a simple comparison between water discharge (84.3×10^6 m^3/year) and water recharge (53×10^6 m^3/year), it can be concluded that the groundwater depletion in Wadi Najran is about 31.3×10^6 m^3/year. The excessive pumping rate reverses the balance

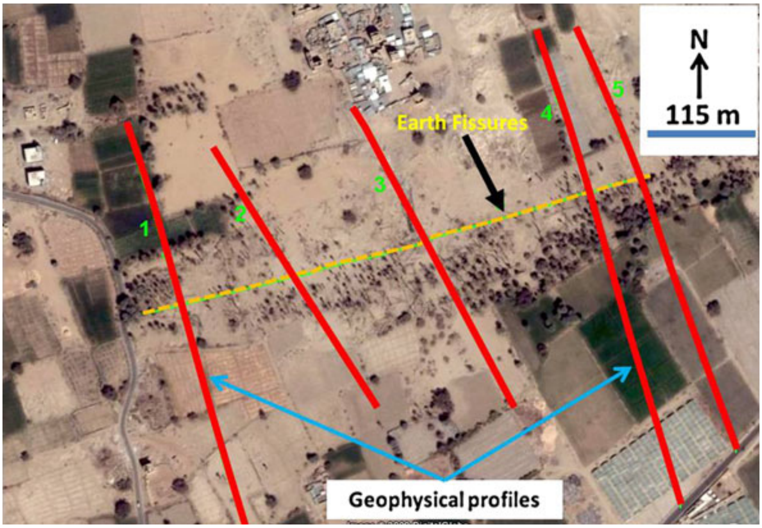

Fig. 7 Electrical resistivity lines along and cross the earth fissure located between agricultural areas

between recharge and discharge (discharge being much greater than recharge). As a result, the water levels in the area continue to decline (Fig. 5).

6.3 Geophysical studies

Geophysical techniques used in earth fissures investigations may include high-resolution seismic reflection, ground-penetrating radar, seismic refraction, magnetic profiling, electrical resistivity, and gravity. Laboratory for advanced subsurface imaging (LASI 2009) studied and tested the capabilities of different geophysical methods including shallow seismic refraction, ground-penetrating radar, electromagnetic resistivity/conductivity, and magnetics for characterization of both an earth fissure and a desiccation crack in an alluvial basin setting of Willcox, Arizona. Rucker and Fergason (2009) conducted a recent subsidence and earth fissure case study and demonstrated the integrated application of InSAR, gravity, electrical resistivity, and refraction microtremor seismic methods for earth fissure characterization.

Part of the current study is to determine the subsurface extent and distribution of earth fissures in the study area. We used an advanced electrical resistivity tomography (ERT) using an IRIS-Syscal Pro resistivity imaging system (96 channels) for this task (to enhance the ability of geophysical exploration, to penetrate to greater depth, and to obtain more detail information). The layout of the geophysical profiles was in the form of five north–south lines (lines 1, 2, 3, and 4, and 5) perpendicular to the earth fissures expressed at the ground surface with an electrode spacing of 5 m (Fig. 7). The electrode configurations employed were reciprocal Wenner Schlumberger, controlled by a laptop computer, which also permitted inversion or modeling of the data in the field. Topographic information was also obtained along each line and was included in the interpreted resistivity models. The following is a brief description of each profile.

Electrical resistivity profile (1): Profile 1 extended for a distance of 390 m (Fig. 7). The surficial reflection of the fissures is quite clear and their extension below the surface is

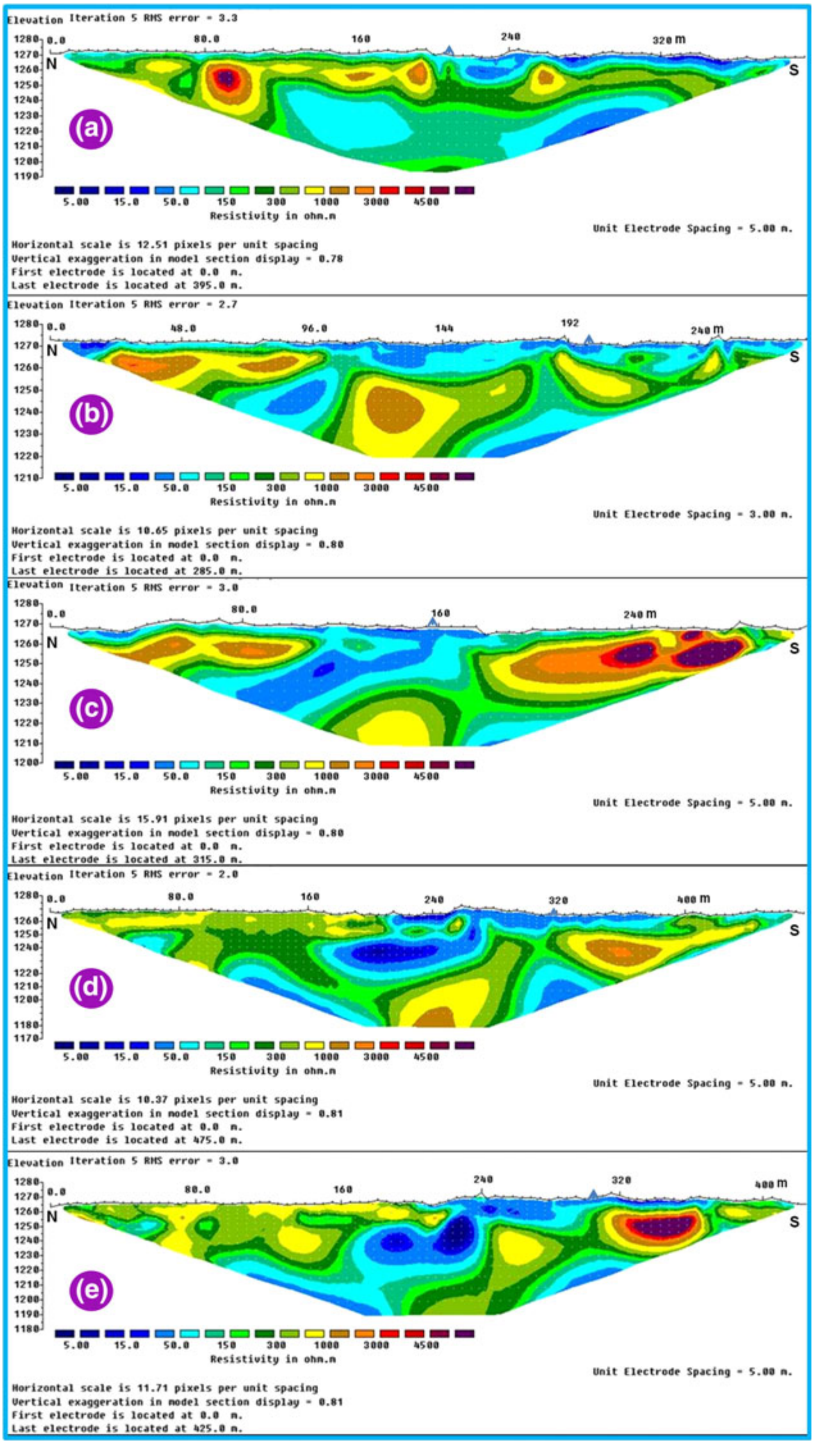
Elevation Iteration 5 RMS error = 3.3
0.0 80.0 160 240 320 m
1280 1270 1260 1250 1240 1230 1220 1210 1200 1190
N
S
(a)
5.00 15.0 50.0 150 300 1000 3000 4500
Resistivity in ohm.m
Unit Electrode Spacing = 5.00 m.
Horizontal scale is 12.51 pixels per unit spacing
Vertical exaggeration in model section display = 0.78
First electrode is located at 0.0 m.
Last electrode is located at 395.0 m.
Elevation Iteration 5 RMS error = 2.7
0.0 48.0 96.0 144 192 240 m
1280 1270 1260 1250 1240 1230 1220 1210
N
S
(b)
5.00 15.0 50.0 150 300 1000 3000 4500
Resistivity in ohm.m
Unit Electrode Spacing = 3.00 m.
Horizontal scale is 10.65 pixels per unit spacing
Vertical exaggeration in model section display = 0.80
First electrode is located at 0.0 m.
Last electrode is located at 285.0 m.
Elevation Iteration 5 RMS error = 3.0
0.0 80.0 160 240 m
1280 1270 1260 1250 1240 1230 1220 1210 1200
N
S
(c)
5.00 15.0 50.0 150 300 1000 3000 4500
Resistivity in ohm.m
Unit Electrode Spacing = 5.00 m.
Horizontal scale is 15.91 pixels per unit spacing
Vertical exaggeration in model section display = 0.80
First electrode is located at 0.0 m.
Last electrode is located at 315.0 m.
Elevation Iteration 5 RMS error = 2.0
0.0 80.0 160 240 320 400 m
1280 1260 1250 1240 1220 1210 1200 1180 1170
N
S
(d)
5.00 15.0 50.0 150 300 1000 3000 4500
Resistivity in ohm.m
Unit Electrode Spacing = 5.00 m.
Horizontal scale is 10.37 pixels per unit spacing
Vertical exaggeration in model section display = 0.81
First electrode is located at 0.0 m.
Last electrode is located at 475.0 m.
Elevation Iteration 5 RMS error = 3.0
0.0 80.0 160 240 320 400 m
1280 1270 1260 1250 1240 1230 1220 1210 1200 1190 1180
N
S
(e)
5.00 15.0 50.0 150 300 1000 3000 4500
Resistivity in ohm.m
Unit Electrode Spacing = 5.00 m.
Horizontal scale is 11.71 pixels per unit spacing
Vertical exaggeration in model section display = 0.81
First electrode is located at 0.0 m.
Last electrode is located at 425.0 m.

◀ **Fig. 8** Electrical resistivity profiles: **a** line 1 length 390 m; **b** line 2 length 290 m; **c** line 3 length 300 m; **d** line 4 length 470 m; and **e** line 5 length 420 m. Note that all profiles start from north and end at south

visible for few meters (Fig. 8a). The earth fissure intersects the profile between 205 and 210 m (Fig. 8a). Figure 8a shows that there is rock at depths less than 5 m with high values of resistivity to the northern side of the profile, while the southern part of the profile is characterized by saturated zone with a relatively low resistivity extending to depths ranging from 10 to 15 m. In addition, there are many high-resistivity zones distributed along this section, and another saturated groundwater zone at below 30 m. It appears that the basement topography is irregular and the overlying sediment has significant thickness variation, this would accelerate the failure rate with further groundwater depletion, and the soil failure will propagate upward toward the surface.

Electrical resistivity profile (2): The length of this line is 300 m (Fig. 7). The earth fissure intersects the profile between 198 and 201 m (Fig. 8b). There are many high-resistivity zones (hard rock) inter-bedded with low resistivity saturated to partially saturated zones. The high-resistivity zones are on the north side at a depth of 7 m and its depth increases toward the south to reach 15–20 m (Fig. 8b). The continuous irrigation of the surrounding fields saturated the upper part of the basin fill for a thickness of 5 m in the north to 15 m in the middle of the profile.

Electrical resistivity profile (3): The length of this line is 300 m (Fig. 7). The earth fissure intersects the profile between 155 and 160 m (Fig. 8c). There are high-resistivity zones in two locations; on the northern side from the beginning of the profile to meter 110, and on the southern side from meter 170 to the end of the profile. The central part of the profile between 110 and 170 m has a thickness of 30–40 m and is a saturated to semi-saturated zone (low resistance). The data show that the earth fissure is at the contact between the hard rock of the southern side and the central sediment layer. It is clear that the bedrock topography and the distribution of sediments play a key role in the fissure formation and the appearance of cracks as the soil consolidates due to water depletion.

Electrical resistivity profile (4): The length of this line is 470 m (Fig. 7). The earth fissure intersects the profile between 315 and 320 m (Fig. 8d). The thickness of a saturated zone at the meter 210 m to 380 along the profile ranges from 10 to 25 m. Bed rock was also detected in different localities where the rock is only 10 m deep between 320 and 450 m. The earth fissure is at the contact between the rock and the sediment layers (Fig. 8d). Again, subsurface topography and the distribution of sediments control the distribution of the soil cracks beneath the surface.

Electrical resistivity profile (5): The length of this line is 470 m (Fig. 7). The earth fissure intersects the profile between points 310 and 315 m (Fig. 8e). The thickness of the soil saturated zone is 10–25 m and encountered between points 210 and 380 m, while bedrock can be interpreted in different locations, getting close to the surface at a depth of 10 m between points 320 and 450 m (southern side of the profile). The earth fissure is at the contact between the hard rock and the sediment layer (Fig. 8e).

7 Conclusions

In order to understand the mode and cause of earth fissure formation, different methods were used including remote sensing, hydrological investigation, and geophysical exploration. The first method indicated that the Wadi Najran area has experience land-use changes of varying degree since 1972. The agricultural areas before 1972 was not more than 47 km^2, but increased to 112 km^2 in 2001. Many additional water wells have been drilled in the Wadi Najran for domestic use and irrigation. With the absence of appropriate management, water pumping is at a rate that exceeds aquifer safe yield, causing a continuous decline of groundwater. Based on the interpretation of the geophysical data, subsurface bed rock forms a buried cliff of steep slopes close to the wadi edge. It was observed in many locations in the five geophysical profiles that earth fissures appeared above the rock slopes; hence, subsurface topography is a key factor for the creation of the earth fissures.

References

Alyamani MS, Hussein MT (1995) Hydrochemical study of groundwater in recharge area, Wadi Fatimah Basin, GeoJournal, Saudi Arabia, Vol. 37. 1, p 81–89

Amin AA (1988) Potential geologic hazards at the village of Tabah, Hail Region. Unpub, MScthesis 164 pp

Amin, AA, Bankher K (1995) Review on land subsidence in Saudi Arabia: in Barends, Brouwer and Schoder (eds.), Land Subsidence, Balkema, Rotterdam, pp 19–26

Amin AA, Shehata WM (1991) Subsidence due to groundwater withdrawal in a volcanic crater, Presented in Hazards '91, Session 11. Perugia, Italy

Arizona Land Subsidence Group (2007) Land subsidence and earth fissures in Arizona Research and information needs for effective risk management: Arizona Geological Survey Contributed Report CR-07-C, 24 p

Bankher K (1996) Engineering geological evaluation of earth fissures in Wadi Al-Yutamah South Al-Madinah Al-Munawwarah, M.Sc. Unpublished thesis, FES, Jeddah (in preparation)

Bell JW, Price JG (1993) Subsidence in Las Vegas Valley, 1980–91–final project report (Open-File Rep. No. 93-4). Reno: Nevada Bureau of Mines and Geology

Bouwer H (1978) Ground water hydrology. International student edition, McGraw-Hill series in water resources and environmental engineering 480 p

Ehret et al. (2007) Numerical modeling of site effects—Influences of groundwater level changes, 1st IASME/WSEAS International Conference on Geology and Seismology (GES'07)

Elsbury RR, Van Siclen DC (1983) Dealing with active surface faulting in Houston: paper presented and distributed at the October 17–21, 1983, ASCE Convention, Houston, Texas

Helm DC (1994) Hydraulic forces that play a role in generating fissures at depth. Bulletin Association Engineering Geologists 31:293–304

Holzer TL (1984) Ground failure induced by ground-water with drawl from unconsolidated sediment. In: Holzer TL (Ed.), Man-induced land subsidence Rev Eng Geol. VI the Geological Soc of America, 67–105

Holzer T, Davis S, Lofgren B (1979) Faulting caused by groundwater extraction in South Central Arizona. J Geophys Res 84(B2):603–612

Laboratory for advanced subsurface imaging (LASI) (2009) Geophysical investigation of subsidence fissures near Willcox, Arizona, Geophysics Field Camp 2009, LASI 09-1, University of Arizona, May 14, available at www.lasi.arizona.edu/GEN%20416%202009%20Final%20Report.doc

Laney RL, Raymond RH, Winikka CC (1978) Maps showing water level declines, land subsidence, and earth fissures in South Central Arizona. U.S. Geological Survey Water Resources Investigation Report 78–83, Scale 1:125,000, 2 sheets

Lofgren BE (1978) Hydraulic stresses cause ground movement and fissures, Picacho, Arizona: Geological Society American Abstracts Programs 10, pp 113

Lund W, Lowe M, Bowman S (2010) Land subsidence and earth fissure policy recommendations. Cedar Valley, Iron County

Medrial A, Kazuhiko Takeuchi, Atsush Tsunekawa (2001) Greenery percentage prediction using RVI, NDVI and MRVI model from Landsat TM and Aerialphoto, in Jabotabek, Indonesia, IECI Japan workshop, Vol.3, No.1, pp 110–113

Mousavi SM, Shamsai A, El Naggar MH, Khamehchian M (2001) A GPS-based monitoring program of land subsidence due to groundwater withdrawal in Iran. Can J Civil Eng 28:452–464

Poland JF (1981) Subsidence in United States due to groundwater withdrawal, J Irrig Drain Div ASCE 107 (IR2), 115–135

Reid WM (1973) Active faults in Houston, Texas (Ph.D. thesis): Austin University of Texas, 122 p

Rucker ML, Fergason KC (2009) Geophysics in geotechnical investigations and mitigations of distressed flood control dams, fast times, Vol 14, No. 1, March, pp 33–42, Published by the Environmental and Engineering Geophysics Society available at http://www.eegs.org/portals/2/fasttimefiles/ft1401_mar2009_low.pdf

Sable EG (1985) Explanation notes on the geologic map of the Najran quadrangle Sheet 17G, Kingdom of Saudi Arabi

Sahu P, Sikdar PK (2011) Threat of land subsidence in and around Kolkata City and East Kolkata Wetlands, West Bengal, India. J Earth System Science 120(3):435–446

Schumann HH (1995) Land subsidence and earth fissure hazards near Luke Air Force Base Arizona In: Prince KR, Galloway DL, Leake SA (Eds.) U.S. Geological Survey subsidence interest group Conference, Edwards Air Force Base, Antelope Valley, California, November 18–19, 1992—abstracts and summary pp. 18–21 Sacramento CA: U.S. Geological Survey. (Open-File Report No. 94–532)

Shanti AM (1993) Geology of the Arabian Shield

Sophocleous M (2000) From safe yield to sustainable development of water resources The Kansas experience. J Hydrol 235:27–43

Sroka A, Hejmanowski R (1991) Pridiction of geometrical changes on the surface and in the rock mass for deep extraction of solid, liquid and gaseous minerals UMM Scientific Bulletins, environmental protection issues series Vol 33

Sun H, Grandstaff D, Shagam R (1999) Land subsidence due to groundwater withdrawal: potential damage of subsidence and sea level rise in southern New Jersey, USA. Environ Geol 37:290–296

Vacher HL, Ayers JF (1980) Hydrology of small oceanic islands: utility of an estimate of recharge inferred from the chloride concentration of the freshwater lens. J Hydrol 45:21–37

Verbeek ER, Ratzlaff KW, Clanton US (1979) Faults in parts of North-Central and Western Houston Metropolitan Area, Texas: U.S. Geological Survey Miscellaneous Field Studies Map MF-1136, scale 1:24,000

Wittaker BN, Reddish DJ (1989) Subsidence :occurrence, prediction and control. DevelopGeotech Eng, 56, Elsevier,528 p

Wolkersdorfer Ch, Thiem G (2006) Ground water withdrawal and land subsidence in Northeastern Saxony (Germany) Mine Water Environ As

Xu YS, Shen SL, Cai ZY, Zhou GY (2008) The state of land subsidence and prediction approaches due to groundwater withdrawal in China. Nat Hazards 45(1):123–135

Zhang Y, Xue YQ, Wu JC, Shi XQ, Yu J (2010) Excessive groundwater withdrawal and resultant land subsidence in the Su-Xi-Chang area, China. Environ Earth Sci 61(6):1135–1143